MEMS Capacitive Accelerometer for Airbag Deployment System

Dante St. Prix
Department of Engineering Physics
University of British Columbia
Vancouver, Canada

I. Introduction

Accelerometers are devices that are designed to measure the acceleration of bodies to which they are attached and output electrical signals proportional to that measurement. These devices are one of the most common applications of MEMS technology. They are used to measure mechanical vibrations in structures, detect earthquakes and have medical applications. In this report, the design process of an in-plane single-axis differential capacitive accelerometer designed specifically for an airbag deployment system in vehicles will be described. This device is designed to be fabricated using the SOIMUMPS® process by MEMSCAP®. This paper will start with a brief theoretical introduction, followed by the specific requirements and previous iterations. Finally, the latest design is presented with results from finite element analysis, system level analysis and a physical network circuit model. A potential readout circuit is included as well. The fabrication masks will be covered in the last section. This design is similar to the design in [1], which boasts a small response to accelerations in other axes which are not being measured.

II. Theory

This type of accelerometer works by measuring the change in distance of a proof mass relative to fixed components in response to an external acceleration. Cantilever flexures are used as springs to provide a force in the opposite direction.

The equation:

$$C = \epsilon_0 \frac{A}{d} \tag{1}$$

relates the capacitance between two conductive plates. ϵ_0 is the dielectric constant of the insulating material between the plates. For air, this value is approximately 8.84×10^{-12}. *A* is the parallel area and *d* is the distance between the two plates. The next equation relates the change in capacitance as a function of its displacement from the original position:

$$\Delta C = C_0 \frac{x}{d_0} \tag{2}$$

x is the displacement and d_0 is the original distance. Using this knowledge, a voltage which is approximately proportional to the distance can be extracted.

A cantilever beam with one fixed end and the other guided has a spring constant of approximately:

$$k = \frac{12EI}{L^3} \tag{3}$$

I is the moment of inertia, which is defined as:

$$I = \frac{wh^3}{12} \tag{4}$$

E is the Young's modulus of the materials, which is around 160GPa for silicon, the material that is used in this device. *h* is the height of the device, *w* is the width and *L* is the length. The spring constant is important as it relates the force that a spring exerts in its linear region to its displacement:

$$F = kx \tag{5}$$

The motion of a mass-spring-damper system is governed by the differential equation:

$$ma(t) = m\frac{d^2x}{dt^2} + b\frac{dx}{dt} + kx \tag{6}$$

a(t) is the external acceleration as a function of time, *m* is the mass of the proof mass, and *b* is the damping constant, which is a function of the viscosity of the surrounding fluid and the geometry of the structure.

In a capacitive mass-spring-damper MEMS device, the distance between the two parallel plates cannot drop below $\frac{2}{3}$ of the initial distance as pull-in will occur past this point. This will short circuit the two plates and damage the device. This is an important factor when determining the spring constant in order to operate within a safe displacement.

III. Design Requirements

This device is designed to meet these requirements:

- Acceleration sensing range: -40g - +40g
- Minimum frequency bandwidth: 0-400Hz
- Minimum resolution: 0.1% of full scale
- Output voltage signal: 0-5V
- Die size: 5×5mm square

The fabrication process imposes these restrictions [2]:

- Device layer thickness: 25μm
- Minimum feature size and spacing between silicon structures: 2μm
- Minimum feature size of oxide structures: 200μm

IV. Previous Attempts

Fig. 1. Several designs were tested before choosing a final one, which does not suffer from the flaws of its predecessors. The first design uses a folded flexure spring in the middle of the device and another cantilever beam connected to a bond pad on the edge of the substrate as shown in Fig. 1. For reference, let us define the x-direction as right-left, the y-direction as up-down and the z-direction as perpendicular to this page. Using AutoDesk Inventor®, it's response to a force in the x-direction was simulated. It showed that the proof mass will rotate about the anchor of the bottom beam as a result of deflection of this beam. Since movement in the y-direction is unwanted, this design cannot be used. To correct this problem, two pairs of identical cantilevers that are parallel to the y-axis should be used. In subsequent iterations, it was found that the comb-fingers (which were 6μm wide, 0

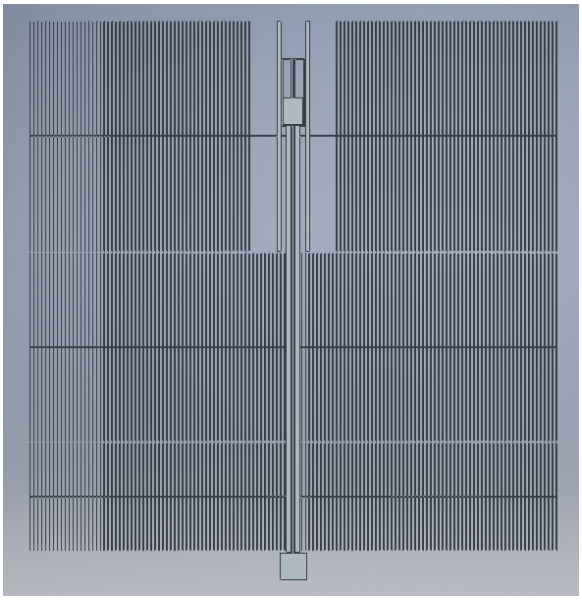

Fig. 1. An image of the proof mass. Not shown in the figure are the fixed capacitive fingers to be placed between each finger of the proof mass. It is designed to sense acceleration in the x-direction. The bottom spring is anchored to the square shaped area on the bottom, where the proof mass connects to a bond pad.

the minimum allowable width in the SOIMUMPS® process) must be wider in order to prevent bending as a result of the force caused by the acceleration. Running static analysis simulations with +40g applied, it was found that beams with a width of 30μm will deflect by a negligible amount. Increasing the width further will benefit the comb-fingers' mechanical properties but will reduce the number of them and thus the capacitance, which is undesirable as parasitic capacitances will have a larger effect on the output voltage and sensitivity will decrease. Finally, having "islands" of silicon dioxide as anchors for the springs is not feasible since one of the fabrication steps involve etching from the bottom of the substrate to reach and etch the silicon dioxide layer; this will cause the release of these "islands".

V. Final Design

Fig. 2 shows the final design of the proof mass and Fig. 3 shows the entire structure of the accelerometer. The proof mass has 36 fingers on each side and is connected to the anchor by 4 parallel 10.75μm wide, 750μm long cantilever springs. It is nearly symmetric in both the x- and y- directions. Each side of the central area containing comb-fingers generates a capacitance with the fixed comb-fingers. The structure moves perpendicular to the fingers.

As it moves in one direction, one of the capacitances decreases while the other increases by the same amount. Four Mechanical stoppers are placed exactly

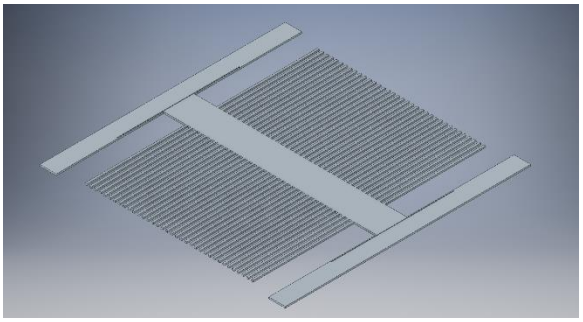

Fig. 2. An image of the proof mass.

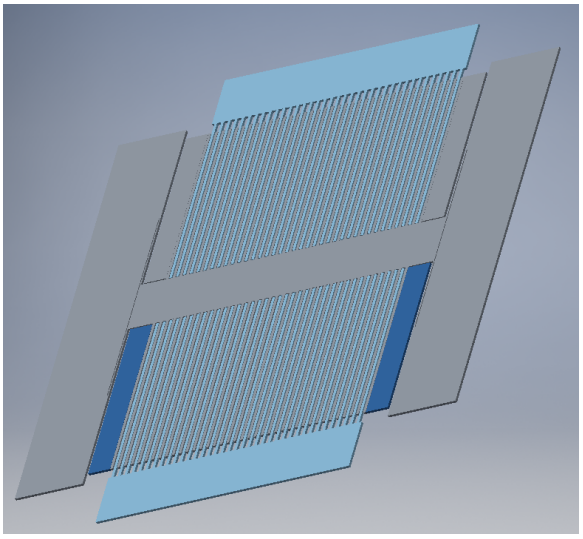

Fig. 3. An image of the entire structure. The grey areas are the proof mass and the top two mechanical stoppers, the light blue areas are the fixed structures and the dark blue areas are the bottom two mechanical stoppers. Three Bond pads (not shown) are placed on the center of the top and bottom fixed structures and on the left anchored section of the proof mass.

2μm from the movable fingers. This ensures that pull-in does not occur.

The mass and initial capacitance of this structure was determined analytically as 314.78μg and 12.44fF respectively. Using the equation:

$$\omega_0 = \sqrt{\frac{k}{m}} \tag{7}$$

the resonant frequency is determined to be 2297Hz.

VI. Finite Element Analysis

Using AutoDesk Inventor®, the spring constant was found by applying various forces and plotting the

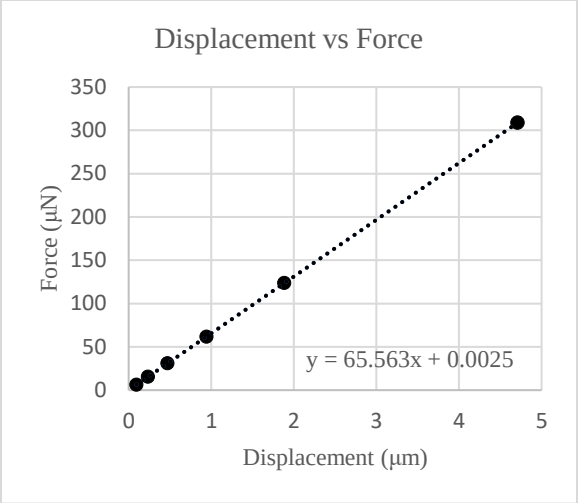

Fig. 4. The data points correspond to forces of 1g, 2g, 5g, 10g, 20g, 40g, and 100g.

force-displacement plot shown in Fig. 4. The spring constant is found to be 65.56N/m. This data also indicates that the springs will remain in their linear region at accelerations far exceeding 40g. By using the formula Eq. (3) the spring constant is analytically determined to be 47.12N/m. 160GPa was used as the value of E. Perhaps the difference is due to the software using another value. In this report, 65.56N/m will be used as the spring constant.

After performing a static analysis with an acceleration of 40g, the displacement was found to be 1.89μm. Using the fact that the spring is linear, the sensitivity ($\frac{\Delta C}{C}$) was calculated to be 0.0079/1g using Eq. (2).

Modal analysis was used to determine the first three resonant modes, plotted in Fig. 5. It is intriguing that the lowest resonant mode is about 1kHz higher than the calculated resonant mode and in a different axis. The third resonant mode at 6kHz is in the desired axis of motion. Although it is unclear why this is the case, since the resonant frequencies are very high, this should not interfere with the operation of the accelerometer. In future iterations, the resonant modes will be studies in more detail.

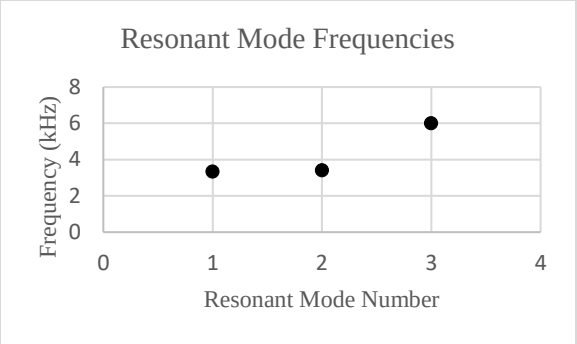

Fig. 5. A plot of the first three resonant modes of the proof mass.

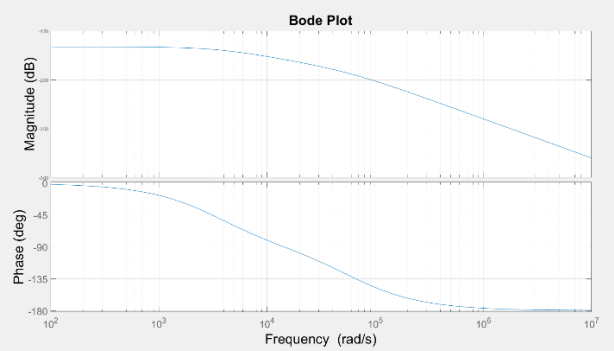

Fig. 6. The Bode Plot of this mass-spring-damper system.

VII. System Level Analysis

Matlab® was used to determine a feasible damping coefficient (b) for the cutoff (3dB) frequency with the requirement being that the cutoff frequency must be at least 400Hz. 20×10^{-3} was chosen as the damping coefficient. Using this value, the cutoff frequency is 450Hz. The Bode Plot of this system is shown in Fig. 6.

Using this value for b, the quality factor Q can be calculated:

$$Q = \frac{\sqrt{km}}{b} \tag{8}$$

Q is calculated to be 0.227.

Using the values for the damping coefficient, spring constant, and mass a Simulink® model was created (Fig. 7) based on Eq. (6).

Fig. 8 and Fig. 9 show change in position of the proof mass and capacitances respectively in response to an acceleration of 1g.

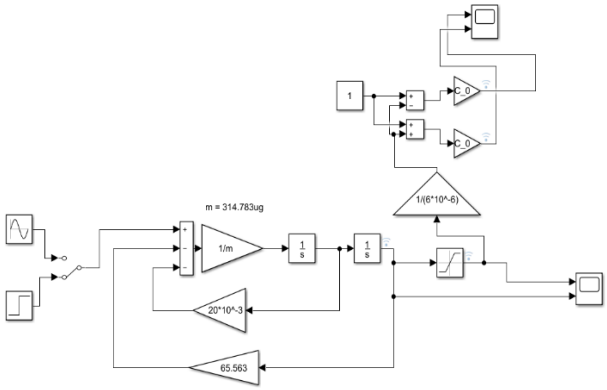

Fig. 7. This Simulink® model displays the proof mass displacement response in the bottom right scope and the capacitance responses in the top right scope.

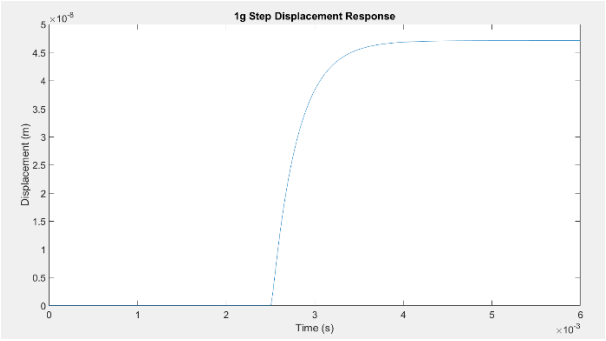

Fig. 8. The 1g step (25ms) displacement response of the proof mass.

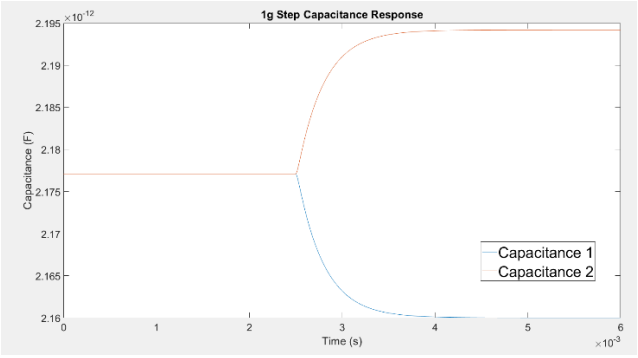

Fig. 9. The 1g step (25ms) capacitance response.

The behavioral model of mechanical stoppers was added to the Simulink® model. Fig. 10 illustrates how when an acceleration of 45g is applied, the mechanical stoppers block the proof mass from moving beyond 2µm. In reality, past 2µm the pull-in effect will cause the displacement to reach d_0, a phenomenon that is not modelled in this study.

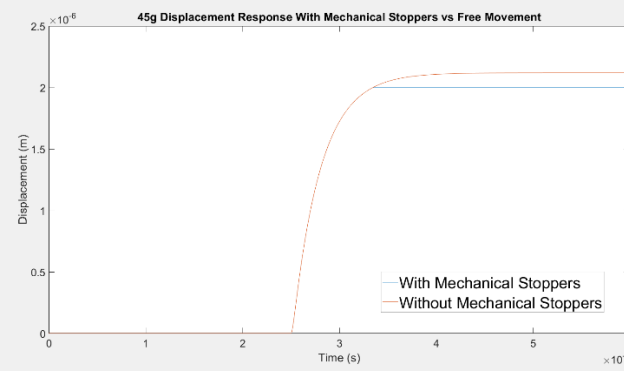

Fig. 10. The 45g step (25ms) displacement response of the proof mass with and without mechanical stoppers.

At this point in the study, most of the parameters for the accelerometer have been determined. Below is a summary table comparing analytical and simulated values:

Table 1 – A comparison of analytical and simulated values.

Value	Analytical	Simulated
Spring Width	10.75µm	
Spring Length	750µm	
Spring Constant (k)	47.12 N/m	65.56N/m
Mass of Proof Mass (m)	314.78µg	N/A
Initial Capacitance (C_0)	12.44fF	N/A
Sensitivity ($\frac{\Delta C}{C}$)	0.0079/1g	
Damping Coefficient (b)	N/A	0.02
Quality Factor (Q)	0.227	

VIII. Physical Network Circuit

A mass-spring-damper system can be modelled as an RLC circuit. Fig. 11 shows the physical network circuit built using Multisim®. The formalism used in this circuit assigns force as voltage. The input voltage (V1) represents the force exerted by the external acceleration. The inductance (L1) is the mass; the resistance of (R1) is the damping coefficient and the capacitance (C1) is 1/k. The voltage across C1 represents the spring force as shown in Eq. (5). Using

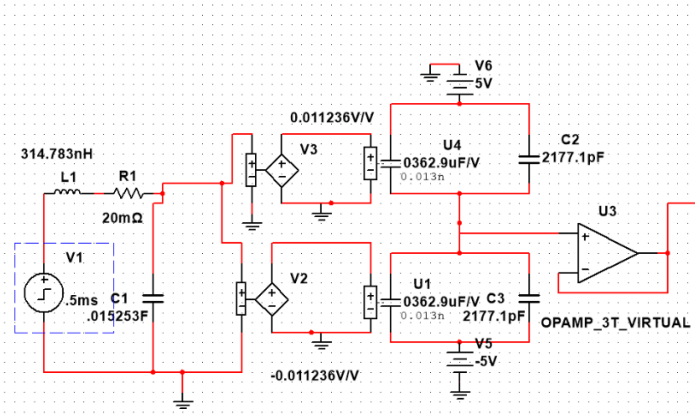

Fig. 11. The physical network circuit representing the mass-spring-damper system of this accelerometer.

an independent voltage source with a gain of 1/k, the displacement (x) can be extracted. Finally, a dependent capacitor was placed in parallel with C_0 to represent the change in capacitance as a function of displacement (one with a positive capacitance and the other with a negative capacitance of the same magnitude). A DC voltage of ±5V is applied to the two capacitors. The voltage of the proof mass (situated between the two capacitors) is the voltage output. A buffer amplifier is added to the output to ensure that signal processing in later stages will not affect the output voltage.

In order for the output voltage to be between 0-5V, a readout circuit is required. 0 and 5V will represent -40 and +40g respectively. Fig. 12 shows the readout circuit. The resistances of R2 and R3 were determined analytically using Eq. (2) and voltage division principles. R2 is used to amplify the output of the previous stage to have a maximum range of 5V. R3 is used to provide a DC offset for the minimum voltage to be 0V. The DC source V4 is negative since this

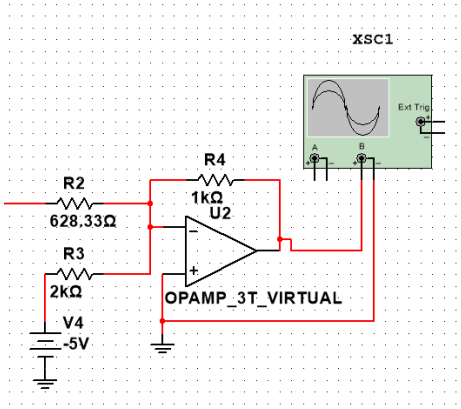

Fig. 12. The readout circuit is comprised of a summing amplifier.

amplifier is an inverting amplifier and a positive voltage output is required. Since an acceleration of 40g causes a 1.89µm displacement of the proof mass. A slightly negative voltage (or voltage above 5V) can be produced with accelerations exceeding ±40g if the operation amplifier can provide such voltages. However, the mechanical stoppers will prevent any voltage corresponding to an acceleration exceeding approximately ±42.3g.

Fig. 13 and Fig. 14 show 1 and 40g step responses (readout voltage) respectively. (It is difficult to read these due to small fonts sizes used by Multisim®. Please refer to the appendix for the magnified figures.) The 1g response of the Simlink® model compliments this finding as both require approximately 2ms to reach their final values. The values are different since the Simlink® model measures capacitance whereas the Multisim® measures the output voltage of the readout circuit. Fig. 15 shows the Bode Plot of the output voltage. The magnitude values of this graph are many orders of magnitude larger than the ones in the Simlink® graph. This is because this graph displays the output voltage whereas the Simlink® graph displays the displacement of the proof mass. However, the cutoff frequencies in both graphs are nearly identical.

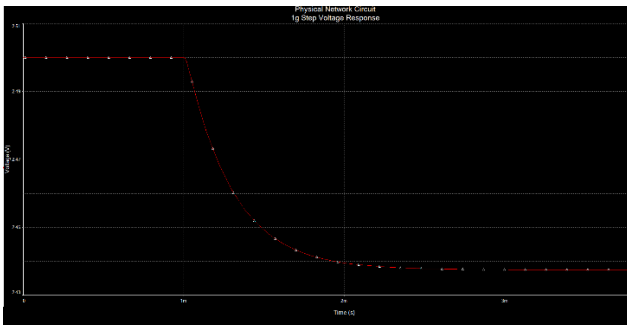

Fig. 13. The 1g step response of the output voltage.

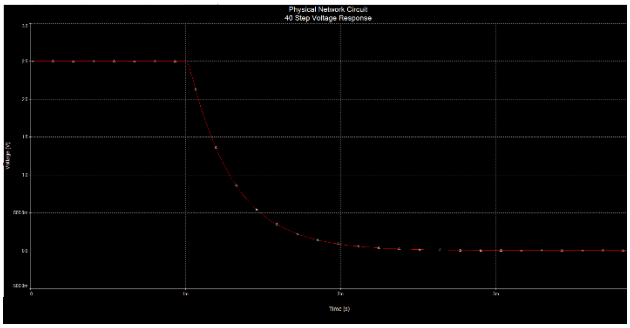

Fig. 14. The 40g step response of the output voltage. This figure demonstrates that a transition from 0g to 40g corresponds to an output voltage from 2.5V to 0V.

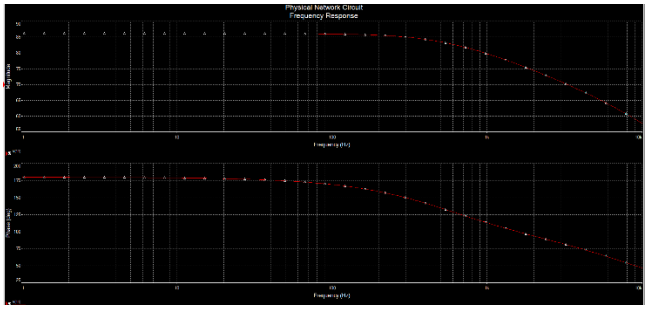

Fig. 15. The Bode Plot of the output voltage of the readout circuit.

In conclusion, the two analyses agree.

IX. Mask Layout

In this section, the masks to be used in the SOIMUMPS® process (generated using Clewin®) are presented. The design rules that are presented in section III of this report are carefully taken into consideration.

Fig. 16 shows the first mask for the pad metal liftoff step. During this step, a layer of chrome (20nm) and gold (500nm) will be deposited on the green areas, which will connect the proof mass, and the two fixed comb drives to the electrical circuit.

Fig. 17 shows the entire mask for the silicon patterning process and Fig. 18 shows a magnified image which displays the small distances between components.

Fig. 19 shows the mask for the substrate patterning from the bottom side of the chip. All features are made to be at least 200µm.

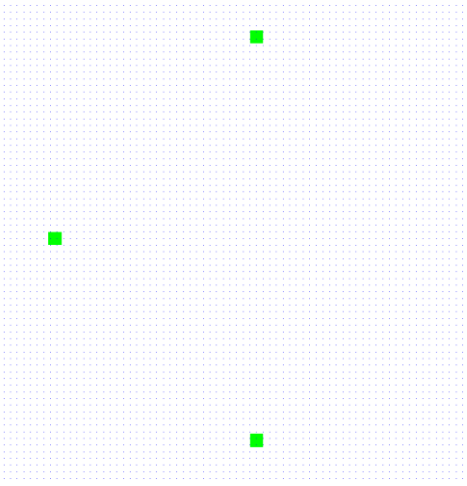

Fig. 16. The photolithography mask for the pad metal liftoff step. It is a clear field mask and intended to be used with positive photoresist.

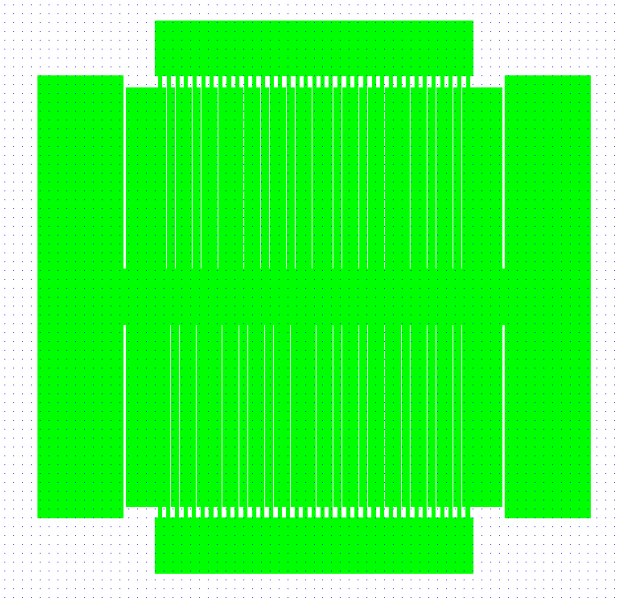

Fig. 17. The mask for the Si Layer. It is a clear field mask and intended to be used with positive photoresist. The dimensions are exactly 5×5mm.

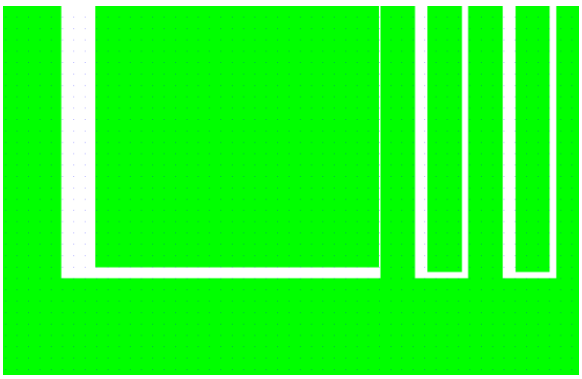

Fig. 18. A magnified image of Fig. 17. The spacing between the mechanical stopper (rectangle in the middle of the image) and the proof mass (to its right) is 2μm, the minimum allowable distance in the SOIMUMPS® process. This also shows how the fingers are closer to one side (6μm) than the other (11.5 μm).

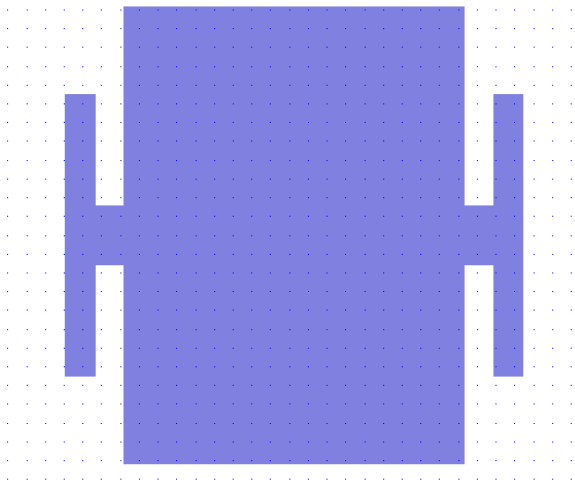

Fig. 19. The mask for the substrate patterning from the bottom side of the chip. This is a clear field mask intended to be used with negative photoresist. All silicon dioxide in the purple area will be removed.

In the last step, a shadow mask process is used to deposit another metal layer. Since no additional metal is required, the shadow mask will cover the entire area of the die.

X. Discussion

The results of the simulations and analytical computations are consistent. One major contradiction was the difference between the spring constant found by AutoDesk Inventor® and the one calculated analytically. For this design to be successful, it is required that both values agree or to have a definitive explanation of which value is correct.

In this design process, the response time and quality factor were not considered as figures of merit. To improve these factors, values for the damping coefficient, the spring constant and mass should be adjusted.

The readout circuit uses very specific resistor values to obtain an output voltage of 0-5V. Current IC technology does not allow such specific values. A solution may be to replace the resistors with diode-connected FET transistors.

Since this process only allows a single device layer, the amount of capacitance per surface area was very limited, which led to low sensitivity. If another process such as PolyMUMPS® were to be used, each proof mass finger can form a capacitance with both fixed areas as illustrated in [1]. They will drastically increase the sensitivity while keeping the area constant.

Although this accelerometer is not yet optimized for production, the results from the system level analysis and physical network circuit show promising results.

XI. References

[1] Sinha, Soumendu & Shakya, Snigdha & Mukhiya, R & Gopal, Ram & D Pant, B. (2014). "Design and Simulation of MEMS Differential Capacitive Accelerometer", VIIth ISSS International Conference on Smart Materials, Strucutures and Systems, July 2014.

[2] MEMSCAP Inc., "SOIMUMPs Design Handbook," 2011.

XII. Appendix

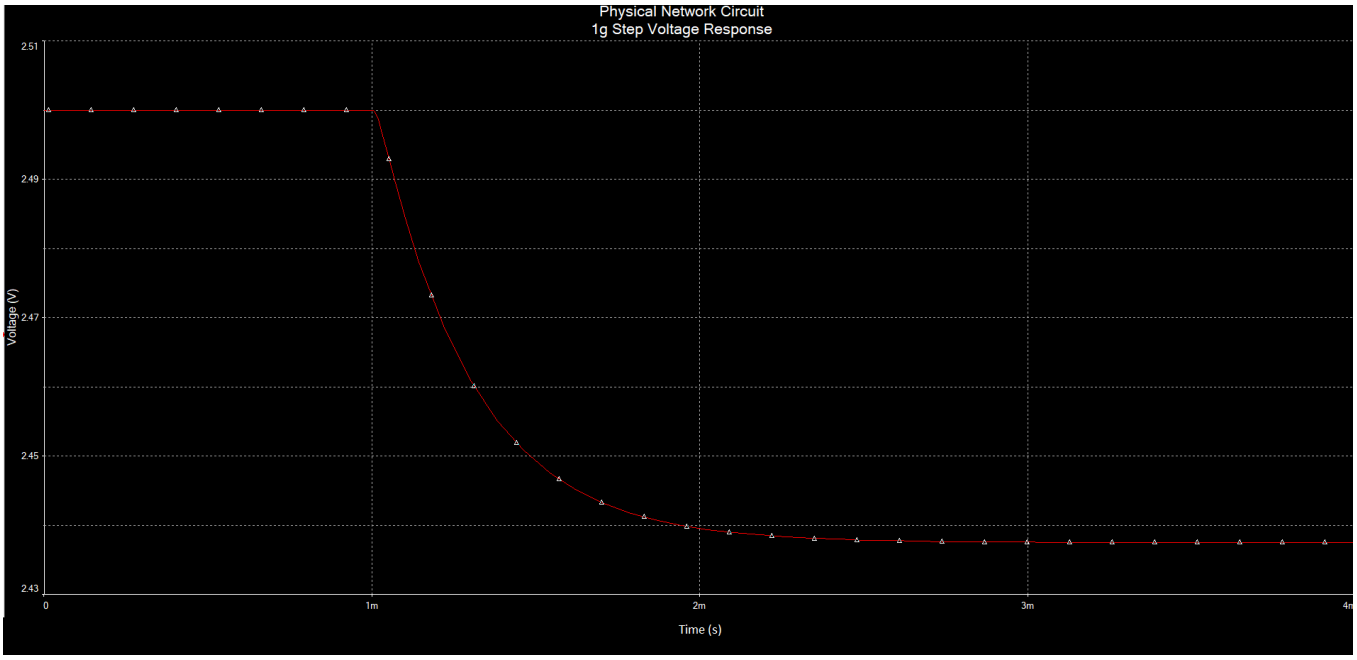

Fig. 13. The 1g step response of the output voltage.

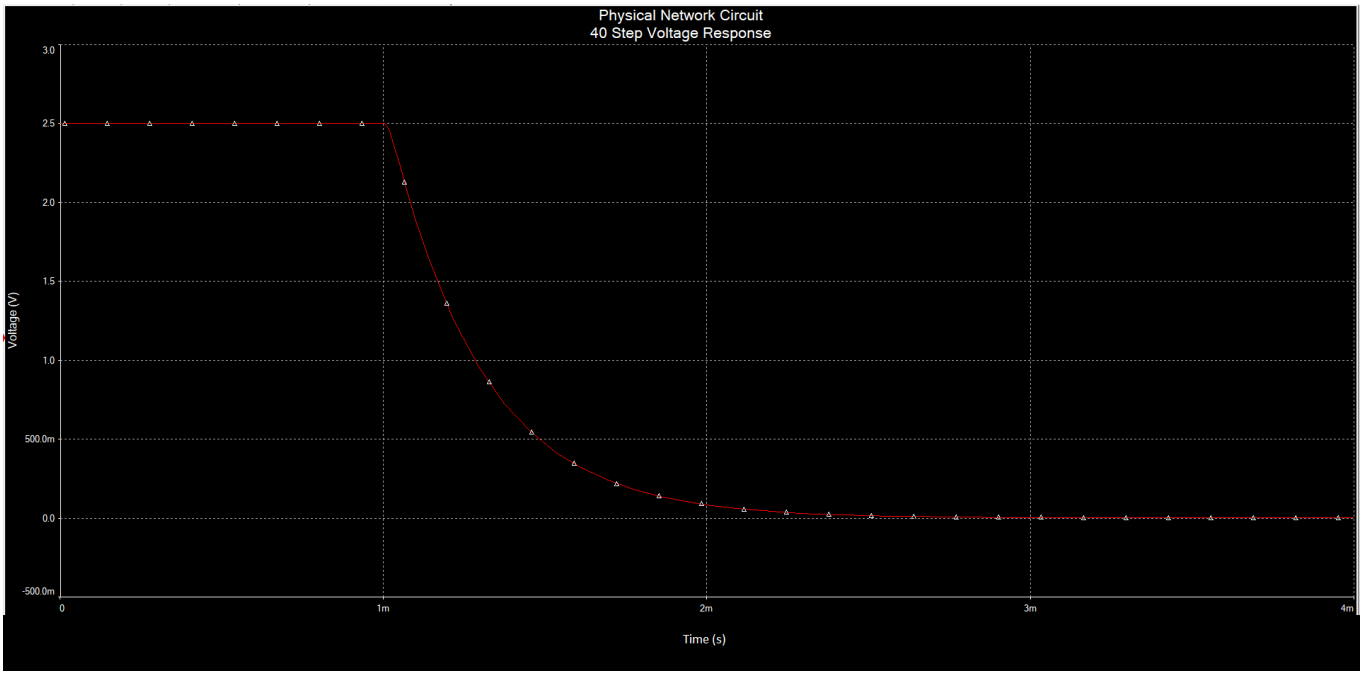

Fig. 14. The 40g step response of the output voltage

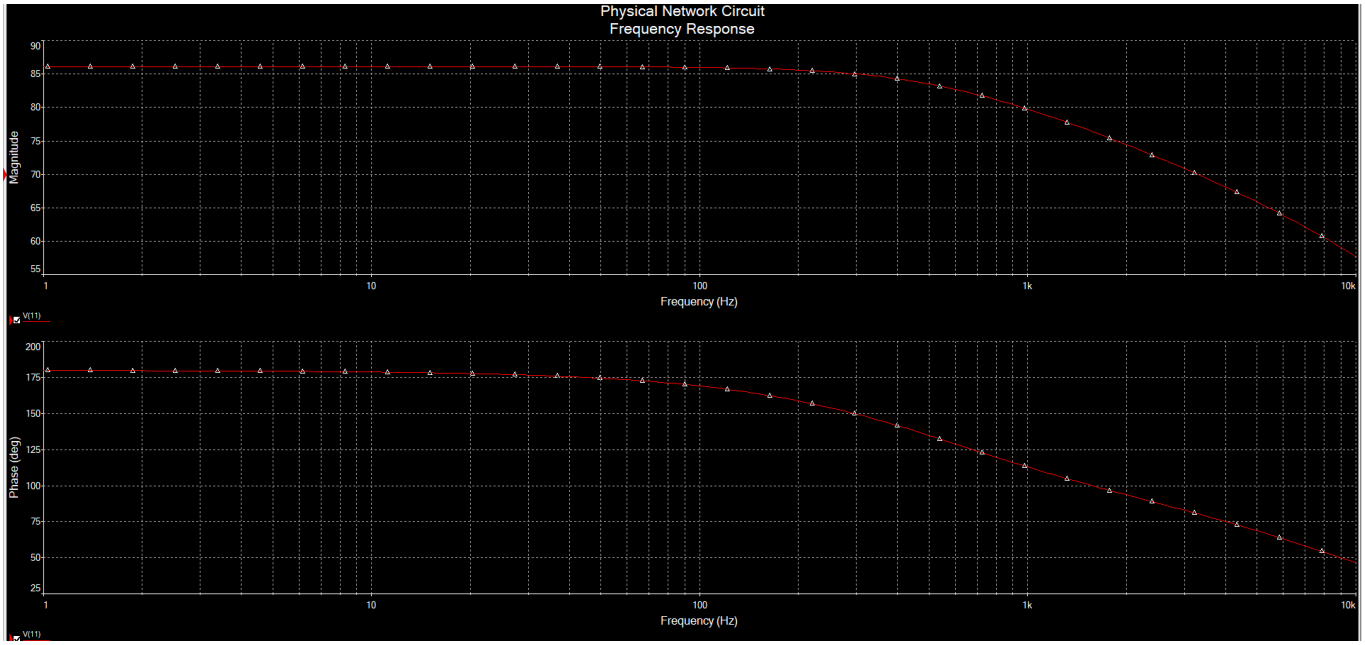

Fig. 15. The Bode Plot of the output voltage of the readout circuit.